



Design, synthesis, and biological evaluation of low-toxic lappaconitine derivatives as potential analgesics

Yuzhu Li^a, Yushan Shang^a, Xiaohuan Li^a, Yinyong Zhang^a, Jiang Xie^b, Lin Chen^{a,**}, Feng Gao^{a,*}, Xian-Li Zhou^{a,b,***}

^a Sichuan Engineering Research Center for Biomimetic Synthesis of Natural Drugs, School of Life Science and Engineering, Southwest Jiaotong University, Chengdu, 610031, PR China

^b Southwest Jiaotong University, Affiliated Hospital, The Third People's Hospital of Chengdu, Chengdu, 610000, PR China

ARTICLE INFO

Keywords:

Diterpenoid alkaloids
Lappaconitine derivatives
Analgesic activity
Toxicity
In-vivo metabolism
Ion channels

ABSTRACT

The C₁₈-diterpenoid alkaloid lappaconitine (LA) is a non-addictive analgesic used in China. The toxicity (LD₅₀ = 11.7 mg/kg) limits its application. Two series of LA derivatives, including amides and sulfonamides (1–93), were designed and synthesized by modification on their C4 acetamidobenzoate side chains in this work. *In vivo* analgesic activity and toxicity of all derivatives were evaluated, and the structure-activity relationship was summarized. Six lead compounds (35, 36, 39, 49, 70, and 89) exhibited approximate analgesic activity to LA but with significantly reduced toxicity. The therapeutic index of these compounds is 14–30 times that of LA. *In vivo* metabolism study of the lead compounds 39, 49, 70, and 89 were conducted by UPLC-MS^E, indicating the reason for the low toxicity of the potential derivatives might be they are difficult to metabolize to toxic metabolite *N*-deacetylappaconitine compared to LA. The effects of lead compounds on sodium channels and hERG channels were also studied by ion channel reader (ICR) which further revealed their analgesic and toxicity-attenuating mechanisms. Sodium channel assay revealed that the analgesic mechanism of these lead compounds was inhibiting the Na_v 1.7 channels. Taken together, compound 39 was provided as a new analgesic lead compound with significantly low toxicity and comparable activity to LA.

1. Introduction

Pain is one of the most common clinical symptoms. According to the International Association for the Study of Pain (IASP), about one-fifth (more than 1 billion) of the world's population suffered from chronic pain of various degrees [1]. Chronic pain seriously affects human physical and mental health and quality of life [2,3], and burdens patients' families and society. Long-term pain could lead to various physical and mental damages such as physiological disorders [4], immunity reduction [5], anxiety [6,7], depression [7–9], and even suicide [9,10].

Medication is still the first choice for treating pain. At present, clinically used analgesics are mainly divided into NSAIDs and opioids (Fig. 1). NSAIDs [11,12], such as aspirin, acetaminophen, ibuprofen, and indomethacin, were widely used for relieving mild aches for their

accurate analgesic activity. However, NSAIDs could cause gastrointestinal adverse reactions [13], kidney [14,15] and platelet function damage [16] and cardiovascular side effects [17,18]. Opioids analgesics represented by morphine, fentanyl, and pethidine are usually μ opioid receptor agonists [19] and are widely used to treat moderate to severe pain [20,21]. Despite their desirable effectiveness, opioids still cause undesirable central nervous system side effects [22,23], as well as addiction [24], analgesic tolerance [25], respiratory depression [26,27], nausea [28], and constipation [29]. Moreover, opioids overdose-related mortality increased exponentially in recent years, mainly because of prescription or illegal use of opioids [30,31]. The fact that pain-afflicted patients around the world lack ideal therapeutic drugs encouraged us to explore new analgesics from traditional Chinese medicine especially the *Aconitum* genus which our team has researched deeply for years.

Caowu, a kind of medicinal plant from the *Aconitum* genus, is

* Corresponding author.

** Corresponding author.

*** Corresponding author. Sichuan Engineering Research Center for Biomimetic Synthesis of Natural Drugs, School of Life Science and Engineering, Southwest Jiaotong University, Chengdu, 610031, PR China.

E-mail addresses: linch@swjtu.edu.cn (L. Chen), gaof@swjtu.edu.cn (F. Gao), zhouxl@swjtu.edu.cn (X.-L. Zhou).

<https://doi.org/10.1016/j.ejmech.2022.114776>

Received 20 April 2022; Received in revised form 11 September 2022; Accepted 12 September 2022

Available online 17 September 2022

0223-5234/© 2022 Elsevier Masson SAS. All rights reserved.

traditional Chinese medicine to cure rheumatic pain [32], sciatica [33], joint pain [34], cancer pain [35], and stomachache [36] in China over thousand years. Two representative plants of Caowu, *Aconitum carmichaelii*, and *Aconitum kusnezoffii Reichb.*, have been recorded in the Chinese Pharmacopoeia to ease rheumatic and relieve pain [37,38]. Modern pharmacological studies proved that the characteristic chemical composition and analgesic ingredient of Caowu are diterpenoid alkaloids [39–42]. Three representative diterpenoid alkaloids, 3-acetylacotinine, bulleyaconitine A, and lappaconitine (LA) (Fig. 1), have been applied in clinical in China for decades due to their remarkable analgesic activities [43–47]. However, diterpenoid alkaloids are also the main toxic component of *Aconitum* spices, which could induce severe side effects such as ventricular arrhythmias, respiratory depression, convulsions, ototoxicity, and allergic reactions even at small dosage [48–54].

LA is a diterpenoid alkaloid isolated from *Aconitum sinomontanum* Nakai. The analgesic effect of LA ($ED_{50} = 3.5$ mg/kg) is seven times that of aminopyrine and is equivalent to morphine and pethidine, leading to LA as an ideal non-addictive drug for the treatment of moderate pain and postoperative pain in cancer patients in China for decades [51]. However, the LD_{50} of LA is 11.7 mg/kg, which is approximate to its ED_{50} (3.5 mg/kg), resulting in a narrow therapeutic window. This disadvantage restricted the extensive use of LA as a more effective analgesic. Thus, modifying lappaconitine to find safer derivatives that combine better analgesic activity and lower toxicity is of considerable importance.

Modification on the side chains of diterpenoid alkaloids would cause obvious changes in their activity and toxicity [55–58]. In our previous study on the chemical composition of *Aconitum apetalum*, a novel diterpenoid alkaloid Apetalrine B (ALB, Fig. 1) with a rare diamino benzamide side chain attached to its C4 position was isolated. To our surprise, ALB is almost none toxic [41], which inspired us to introduce its unique side chain into the structure of LA, hoping to reduce its toxicity. Thus, two LA derivatives (16 and 18) were synthesized in the preliminary study and their LD_{50} exceeded 100 mg/kg. Recently, it has been reported that LA could ease pain by directly stimulating dynorphin A expression in spinal microglia, while their toxicity was caused by the interaction with voltage-gated sodium channels [45,46,59]. The newly illustrated theories, together with the reduced toxicity of compounds 16 and 18, indicated that the toxicity and antinociception of diterpenoid alkaloids might follow different mechanisms and could be separated through rational structural modification.

In the present work, inspired by the unique structure of a low toxicity diterpenoid alkaloid we discovered before [41], ninety-three LA analogues, including amides series and sulfonamides series, were designed

and synthesized, in which six potential lead compounds were derived by analgesic activity and toxicity screen *in vivo*. These six compounds kept the analgesic activity comparable to that of LA and exhibited significantly reduced toxicity. The therapeutic index (TI) of the lead compounds was 14–30 times higher than that of LA. Furthermore, a clear Structure-Activity Relationship (SAR) of all the LA derivatives has been summarized to guide further modification of diterpenoid alkaloids. The *in vivo* metabolic fate of the leading compounds was conducted by UPLC-MS^E to reveal the possible toxicity-attenuation mechanism, and the effect of the lead compounds on the sodium channels and hERG channels was also studied. Based on the above results, our work provided compound 39 as the optimal LA derivative that exhibited significantly reduced toxicity while maintaining the analgesic activity comparable to LA.

2. Results and discussion

2.1. Chemistry

As shown in Scheme 1, inspired by the structure and low toxicity of ALB, two series of LA derivatives, amides, and sulfonamides, were designed and synthesized. Keeping the amide fragment in LA unchanged, three types of LA amide derivatives were designed according to the difference in R group, including alkyl, heterocyclic, and phenyl groups, respectively. As isostere of amide structures, sulfonamide fragments have been used in various leading compounds and drugs [60,61]. The facts inspired us to transform the amide in LA into sulfonamide. Similarly, three classes of derivatives were designed and synthesized depending on the difference of R substituents, which were alkyl, heterocyclic, and phenyl groups, respectively.

The target compounds were synthesized according to the steps outlined in Scheme 1. By the method described in the literature [60], *N*-deacetylappaconitine (DLA) was prepared by acid hydrolysis of LA in satisfactory yields. The designed compounds were synthesized by amidation or sulfonamidation of *N*-deacetylappaconitine with commercially available or synthesized acyl chlorides or sulfonyl chlorides. The structures of isolated products 1–93 were established based on their NMR spectral analysis.

2.2. Pharmacology

Using LA as a positive control, all the LA derivatives prepared herein were screened for their *in vivo* analgesic activities (Table 1), performed

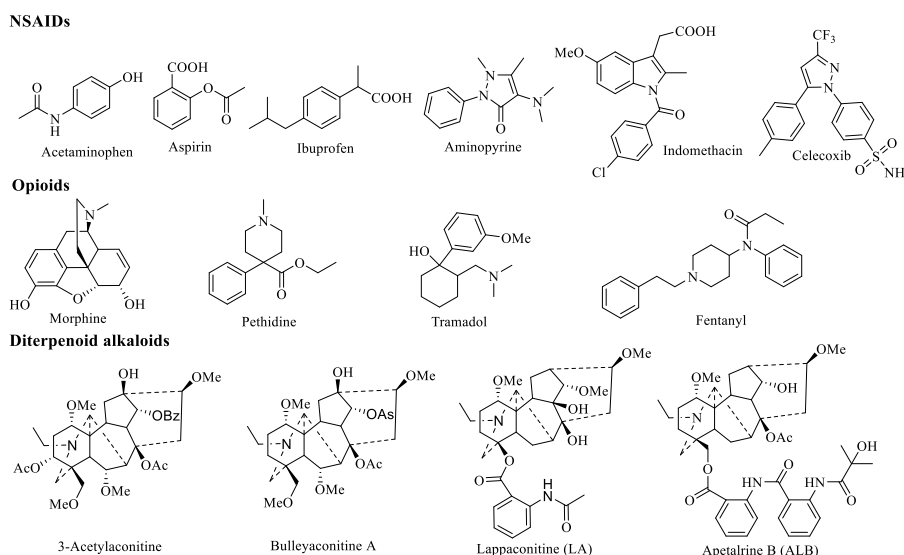
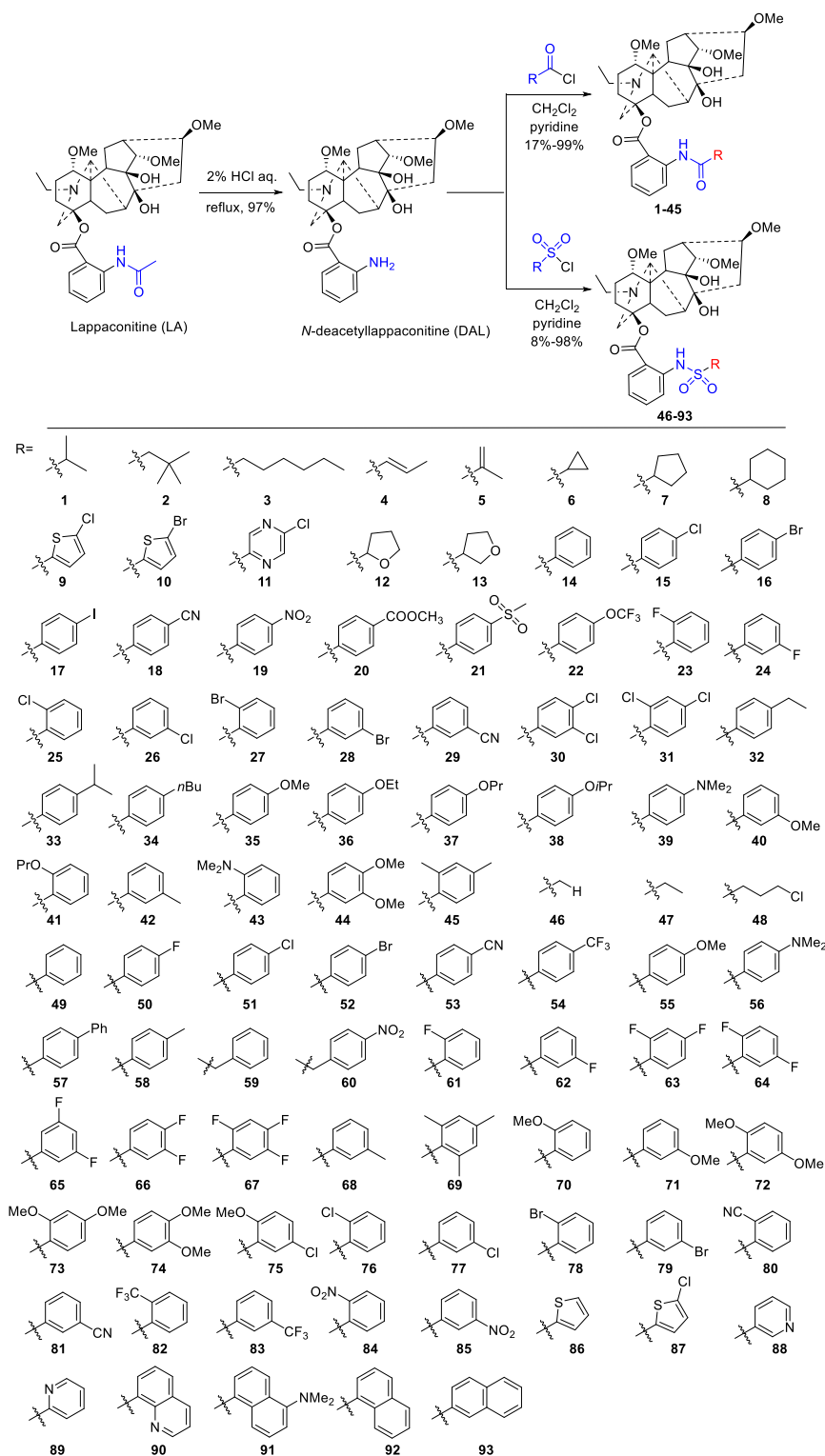


Fig. 1. Representative NSAIDs, opioids, and diterpenoid alkaloids.



Scheme 1. Synthesis of LA Derivatives.

by the classic acetic acid-induced mice writhing test. For compounds with better activity (inhibition rate >60%), the median effective dose (ED₅₀), median lethal dose (LD₅₀), and therapeutic index (TI) were determined and calculated. The SAR of derivatives from the two series were analyzed and summarized.

The most significant feature of alkyl-substituted derivatives of amide series is their high toxicity. The toxicity of alkyl-substituted compounds with fewer carbon atoms in R (compounds 1, 4-6) was equivalent to that

of LA (LD₅₀ = 11.7 mg/kg), while decreased as the number of carbon atoms in R increased. Compounds 2, 3, 7, and 8 did not cause animal death at the dosage of 10 mg/kg. However, when the dose increased, these four compounds gradually caused poisoning reactions including twitching of limbs, foaming at the mouth, and lip bruising, and half of the tested mice (*n* = 10) were dead at the dosage of 100 mg/kg in 24 h.

Unfortunately, the heterocyclic-substituted amide derivatives exhibited low inhibition rates. 2-chloro-thiophene-substituted

Table 1
Writhing inhibition (%) of LA derivatives (dosage 10 mg/kg)^a.

No.	Inhibition (%)	No.	Inhibition (%)	No.	Inhibition (%)	No.	Inhibition (%)
LA	— ^b	22	10.0 ± 11.5	47	4.0 ± 9.5	72	65.8 ± 4.1*
	56.6 ± 6.6* ^c	23	17.7 ± 7.9	48	32.1 ± 5.9*	73	34.9 ± 5.5*
1	— ^b	24	27.5 ± 6.3*	49	84.3 ± 3.1*	74	13.7 ± 18.5
2	24.9 ± 9.7 ^c	25	4.4 ± 10.4	50	14.7 ± 13.2	75	43.2 ± 7.5*
3	54.2 ± 6.2*	26	17.5 ± 11.9	51	11.7 ± 7.8	76	64.3 ± 7.1*
4	— ^b	27	0.0 ± 7.5	52	11.4 ± 7.6	77	33.1 ± 4.6*
	24.4 ± 8.5* ^c	28	3.4 ± 15.3	53	21.4 ± 7.5*	78	24.7 ± 9.1
5	— ^b	29	10.7 ± 7.3	54	19.4 ± 5.0	79	13.0 ± 7.8
6	— ^b	30	10.4 ± 7.3	55	16.8 ± 6.1	80	53.9 ± 7.1*
	33.5 ± 7.3** ^c	31	31.2 ± 3.7*	56	23.0 ± 8.8	81	47.4 ± 4.6*
7	56.9 ± 3.8*	32	26.7 ± 8.0	57	16.1 ± 10.6	82	55.2 ± 8.4*
8	34.5 ± 4.7*	33	21.0 ± 6.6	58	27.7 ± 12.9*	83	12.8 ± 9.8
9	27.8 ± 5.8	34	28.2 ± 7.9	59	43.8 ± 4.5*	84	58.5 ± 7.9*
10	12.8 ± 13.4	35	62.8 ± 5.8*	60	42.4 ± 6.0*	85	6.7 ± 6.1
11	31.5 ± 8.2**	36	62.8 ± 5.4*	61	60.3 ± 5.9*	86	1.0 ± 5.4
12	21.8 ± 12.6	37	48.4 ± 6.1*	62	50.2 ± 6.9*	87	31.3 ± 7.7**
13	34.0 ± 8.9*	38	51.1 ± 5.5*	63	27.2 ± 4.9*	88	32.3 ± 8.2**
14	0.0 ± 11.0	39	62.1 ± 5.0*	64	45.1 ± 5.4*	89	71.2 ± 2.7*
15	31.6 ± 12.6	40	0.0 ± 13.4	65	37.5 ± 7.6*	90	42.4 ± 6.0*
16	39.4 ± 7.2*	41	19.2 ± 17.6	66	28.3 ± 6.7*	91	42.5 ± 2.6*
17	31.1 ± 8.6	42	36.9 ± 9.4*	67	26.0 ± 19.2	92	49.3 ± 5.0*
18	31.5 ± 10.3**	43	34.2 ± 5.1**	68	52.1 ± 11.0*	93	28.4 ± 9.5**
19	27.2 ± 11.0	44	34.6 ± 6.4*	69	52.1 ± 5.3*		
20	36.4 ± 9.5	45	0.0 ± 11.0	70	71.2 ± 3.8*		
21	8.4 ± 12.7	46	22.8 ± 7.6**	71	37.1 ± 15.7*		

^a Values are expressed as the mean ± SEM.

^b The writhing inhibition could not be calculated due to the animals died at 10 mg/kg.

^c Tested dosage 3.5 mg/kg *p < 0.01, **p < 0.05.

compound **9** exhibited higher inhibition than 2-bromo-thiophene-substituted **10**, indicating the size of the halogen atoms on the thiophene ring may have an impact. The writhing inhibition of compound **13** is about 10% higher than that of **12**, suggesting the distance between the oxygen atom and the carbonyl group may affect the analgesic activity in tetrahydrofuran-substituted derivatives. These derivatives did not cause any obvious toxic symptoms or death at the measured concentration (10 mg/kg), indicating that their toxicities had been reduced to some extent compared with LA. As the activities of heterocyclic-substituted derivatives were generally low, their toxicity was not studied.

Phenyl-substituted amide derivatives showed various analgesic activities according to the multiple substituents on the phenyl ring. The analgesic effect of benzene substituted compound **14** almost disappeared. Generally, the introduction of phenyl ring with *para*-electron-donating groups such as alkoxy and *N,N*-dimethylamino groups (**35–39**) showed better inhibition than *para*-electron-withdrawing groups (**15–22**). But the introduction of phenyl ring with *para*-alkyl groups (**32–34**) has similar inhibition rates to *para*-electron-withdrawing groups. When substituents were installed at the *ortho*-position or *meta*-position, the inhibition was reduced compared to *para*-substituted (**23–29**, **40–43**). Similarly, the activities of disubstituted phenyl rings also dropped the writhing inhibition. In summary, the inhibition was enhanced when electron-donating groups (alkoxy and *N,N*-dimethylamino groups) were installed at the *para*-position of the phenyl ring. Among these compounds, the inhibition of **35**, **36**, and **39** were all above 60%. Compounds **37** and **38** with *n*-propoxy and isopropoxy groups exhibited inhibition of around 50%. The inhibition rates of **37–38** were about 10% lower than that of **35** and **36**, suggesting that the activities of these compounds gradually decreased with the extension of the alkoxy carbon chain.

As shown in Table 1, the alkyl-substituted derivatives in the sulfonamide series did not exhibit satisfactory activities at 10 mg/kg (**46–48**). Moreover, these compounds all caused poisoning reactions such as twitching and difficulty breathing in mice at testing concentrations. But the toxicity is not as significant as that of alkyl-substituted amide derivatives.

The phenyl substituted sulfonamide derivatives exhibited a different SAR from the amide series. Unlike **14**, compound **49** with a benzene ring substituted displayed the highest inhibition rate (84.3%) among all compounds. Both phenyl rings with *para*-electron-withdrawing and *para*-electron-donating groups showed low inhibition rates (**50–58**). The inhibition rates of benzyl substituted compounds (**59–60**) were slightly higher than that of compounds **50–58** but weaker than that of compound **49**. All *ortho*-substituted phenyl sulfonamide derivatives except *ortho*-bromo-phenyl have moderate to good inhibition rates through 53.9–71.2% (**61**, **70**, **76**, **78**, **80**, **82**, and **84**). When substituents were installed at the *meta*-position, compounds with fluorine, methyl, and cyano groups behaved at moderate inhibition rates (**62**, **68**, and **81**). Still, compounds with methoxy, fluoro, bromo, and nitro groups (**71**, **77**, **79**, and **85**) reduced the inhibition rates. Compared with amide derivatives, the locations of substituents played a more significant role than substituents themselves (Fig. 2). All sulfonamide derivatives with *ortho*-substituted phenyls showed better inhibition rates than those with *meta*-substituted phenyls when they had identical substituents (**61**, **70**, **76**, **78**, **80**, **84** vs. **62**, **71**, **77**, **79**, **81**, **85**, respectively). 2,5-disubstituted phenyls no matter with electron-donating (methoxy, **72**) or electron-withdrawing (fluoro, **64**) groups have better inhibition rates than 2,4/3,5/4,5-disubstituted compounds (**63**, **65**, **66**, **73**, and **74**). When

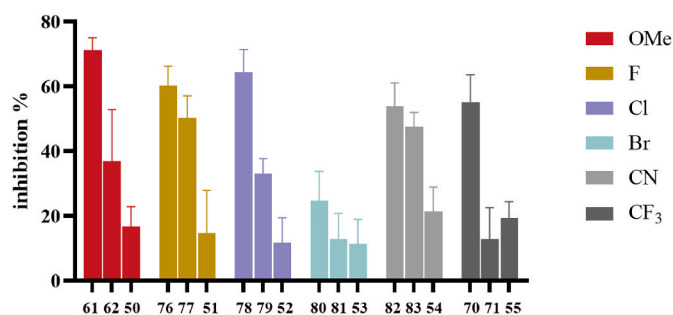


Fig. 2. Comparison of inhibition rates of phenyl-substituted derivatives in sulfonamide series with identical substituents on different positions.

heteroaryl groups were introduced, the 2-pyridyl group enhanced the inhibition rate to 71.2% (**89**), whereas the inhibition rates of others were 1.0–42.4% (**86–88, 90**). The introduction of the naphthalenyl group did not benefit inhibition rates (**91–93**).

To further study the analgesic potency, selected compounds with inhibition rates over 60% (**35, 36, 39, 49, 70, 89**) were further tested for median effective dose (ED₅₀) by the classic acetic acid-induced mice writhing test, using LA as a positive control. The results are shown in Table 2. The analgesic efficacy of **35, 36, 39, 49, 70** and **89** (ED₅₀ = 4.4, 6.6, 6.2, 6.1, 5.5 and 4.7 mg/kg, respectively) were equivalent to that of positive control drug LA (ED₅₀ = 3.5 mg/kg). The activities of **37** and **38** (ED₅₀ = 10.2 and 8.1 mg/kg, respectively) were slightly lower than that of LA, but it is also in the same order of magnitude.

Toxicity is the most significant problem of LA. The aim of this study is to find LA derivatives with lower toxicity. Since compounds **35–39, 49, 70**, and **89** exhibited similar ED₅₀ to LA, their median lethal dose (LD₅₀) was further determined by the acute toxicity test. The LD₅₀ of compounds **35, 36**, and **39** were 296.4, 314.7, and 300.0 mg/kg, respectively, nearly 30 times that of LA (LD₅₀ = 11.7 mg/kg), indicating their toxicity was significantly reduced after structure modification. The toxicity of **37** and **38** was also decreased (LD₅₀ = 213.6 and 195.8 mg/kg) nearly 20 times of LA. Surprisingly, compound **49** did not cause animal death at 600 mg/kg within 24 h. Limited by its solubility, the LD₅₀ data of **49** cannot be measured, which means the toxicity of compound **49** is far lower than LA and selected compounds in the amide series (**35–39**). The LD₅₀ of sulfonamide derivative **70** (300.0 mg/kg) was equivalent to compounds **35, 36**, and **39** in the amide series. The LD₅₀ of **89** was over 400 mg/kg and cannot be measured because of the solubility. Compounds **35, 36, 39, 49, 70**, and **89** exhibited the same analgesic activity as LA but a far better therapeutic index (Table 2), suggesting they might be safer analgesic lead compounds.

We also conducted preliminary toxicity screening for other phenyl-substituted derivatives, including compounds **14–22, 27–29, 40**, and **43**. These compounds did not cause any obvious toxic symptoms or animal death at 100 mg/kg, which means their toxicity was reduced significantly. The results indicated that phenyl substituents of the side chain in the C4 position of LA might play a key role in reducing the toxicity of LA.

2.3. *In vivo* metabolism study of compounds **39, 49, 70** and **89**

To further understand the poisonousness-attenuated mechanisms and the metabolic fate of the above-mentioned LA derivatives, we conducted *in vivo* metabolism study of representative compounds **39, 49, 70**, and **89** (parent drugs marked as A, B, C, and D, respectively) by UPLC-MS^E and the data was processed by UNIFI software to identify the possible metabolites of these LA derivatives.

2.3.1. Mass spectral fragmentation of compounds **39, 49, 70**, and **89**

Since the mass fragmentation patterns of the metabolites were similar to the parent drug, a better explanation of the parent compound fragmentation patterns would be beneficial for metabolite

Table 2
Activity and toxicity of selected compounds.

Compounds	ED ₅₀ (mg/kg)	LD ₅₀ (mg/kg)	TI
LA	3.5	11.7	3.3
35	4.4	296.4	67.4
36	6.6	314.7	47.7
37	10.2	213.6	20.9
38	8.1	195.8	24.2
39	6.2	300.0	48.5
49	6.1	>600 ^a	>98.3
70	5.5	300.0	54.5
89	4.7	>400 ^a	>85.1

^a The LD50 cannot be determined due to the solubility of compounds.

characterization. As shown in Fig. 3, the parent compounds were analyzed by MS/MS in the ESI positive ionization mode to obtain the fragment ions. The fragmentation pathways were proposed (Supporting Information, Table S1, and Fig. S96) to guide the structure elucidation of the metabolites.

2.3.2. Metabolic fate of LA derivatives **39, 49, 70**, and **89**

All the urine and feces samples were subjected to UPLC-Q/TOF-MS^E, and the total ion chromatogram peaks (Supporting Information, Fig. S95) were analyzed using software UNIFI to provide information for all possible metabolites. Based on the results of UNIFI and further MS/MS fragmentation behavior of parent drugs, the metabolites were deduced. Sixteen, fourteen, twenty-two and nine metabolites were identified from compounds **39, 49, 70**, and **89** (Supporting Information, Tables S2–S5 and Fig. S96). Similar to the *in vivo* metabolic pathway of LA, the four lead compounds obtained in this study were mainly metabolized in phase I, and the major metabolic reactions included hydroxylation, O-demethylation, N-deethylation, dehydrogenation, and the hydrolysis of amides, sulfonamides, and esters. To better understand the metabolisms of these four compounds *in vivo*, the amount of the metabolites was determined based on their response value. The relative percentage of all metabolites in urine and feces were shown in Fig. 4.

In previous studies, the primary metabolites of LA were deduced to be the N-deacetylated ones, including N-deacetylappaconitine (DAL), N-deacetyl-O-demethylappaconitine (DMDAL), and the hydroxylation or O-demethylation metabolites of DAL and DMDAL. The content of DAL was more than double that of LA [62,63]. These facts suggested that the amide bond in the structure of LA was unstable *in vivo* and could be easily broken by the metabolic reaction to form DAL. However, in this study, the amount of DAL was meager. Compounds excreted in urine and feces were mainly in their original form and the primary metabolites basically maintained the modified structure unchanged. Considering the toxicity of DAL was comparable to that of LA, it could be concluded that DAL is the primary toxic metabolite of LA. Compounds that were more easily metabolized to DAL *in vivo* exhibited higher toxicity. Phenyl-substituted derivatives from the amide series generally showed significantly reduced toxicity because the introduction of the benzene ring made the amide bond difficult to be metabolically cleaved *in vivo*. Moreover, since sulfonamide bonds exhibited stronger stability than amide bonds, the toxicity of phenyl-substituted derivatives from sulfonamide series such as compounds **49** and **89** were further reduced.

2.4. Effect of the lead compounds on voltage-gated sodium channels (Na_v 1.7)

As an important class of transmembrane proteins, voltage-gated sodium channels (Na_vs) play a crucial role in the generation and transmission of action potentials in excitable cells such as nerve cells, muscles, and heart tissues. Among the nine subtypes of human voltage-gated sodium channels, Na_v 1.7, which is highly expressed in peripheral sensory neurons, has a direct association with pain syndrome [64,65]. It is reported that LA exerts analgesic activity because of it is a Na_v 1.7 inhibitor [66]. Since our leading compounds exhibited analgesic activity comparable to LA, their effects on Na_v 1.7 were further explored to explain their analgesic mechanism.

Herein, using Li⁺ as a tracer ion (with a maximum absorption peak at 670.8 nm), after adding a sample buffer containing a certain concentration of compounds to the cultured HEK-Na_v 1.7 cells and incubating for a period of time, a high concentration of Li⁺ buffer was added to the cells and incubated for a period of time to make Li⁺ enter the cells. The cell lysate (intracellular fluid) was collected and the Li⁺ concentration was tested using an ion channel reader (ICR 8100, Aurora, Canada). The Li⁺ concentration in cell lysate could reflect the effects of tested compounds on Na_v 1.7. As shown in Table 3 and Fig. 5, all of the lead compounds exhibited inhibition on the Na_v 1.7 channels at 100 μM. Compounds **35** and **39** from the amide series could inhibit the channels

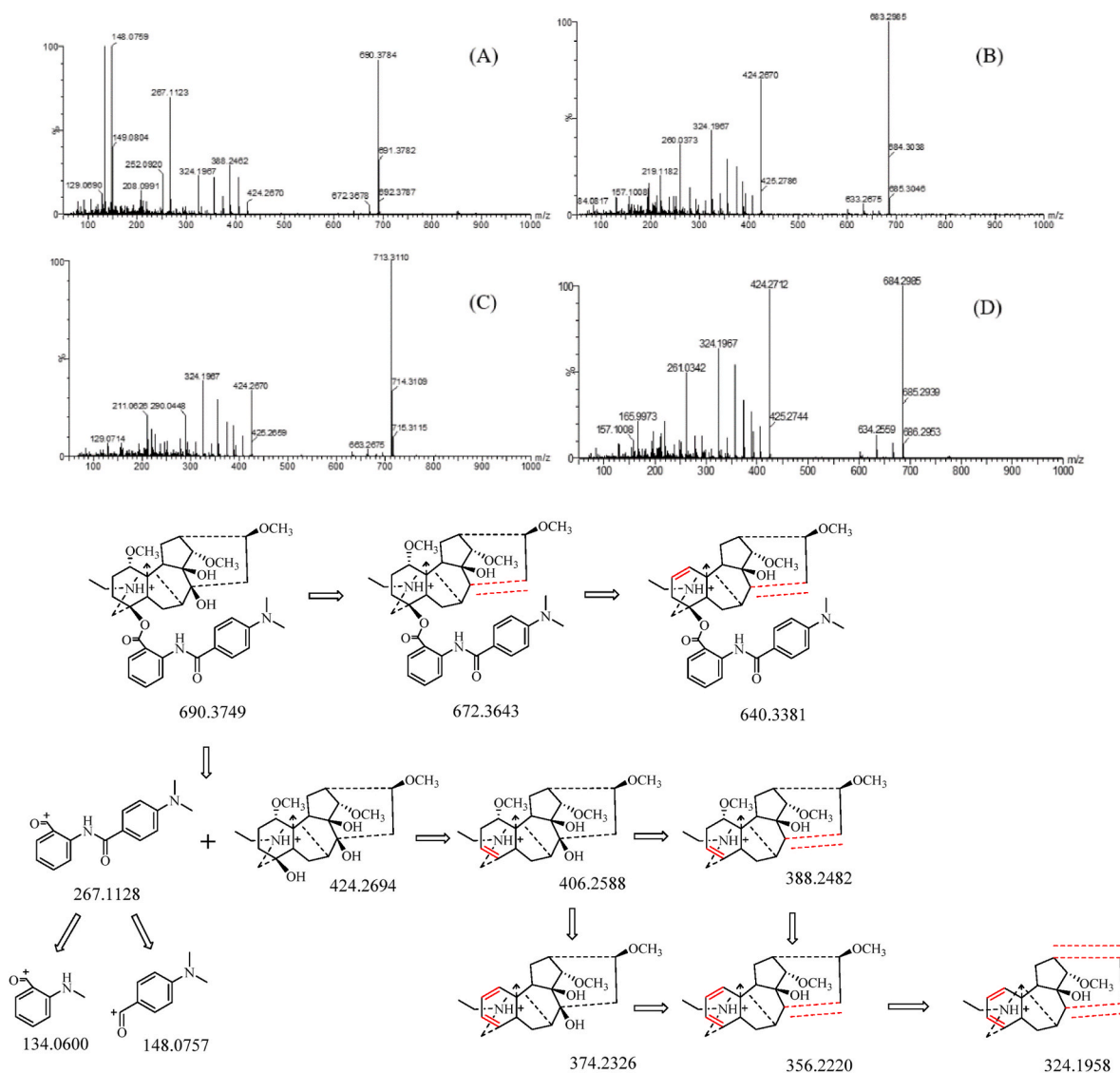


Fig. 3. The accurate MS/MS spectral of compounds **39** (A), **49** (B) **70** (C), and **89** (D) and the proposed fragmentation pathway of compounds **39** parent ion [M + H]⁺. Pathways of the other compounds were shown in Supporting Information Fig. S96.

at 10 μ M, suggesting that the mechanism of the lead compounds was the same as that of LA, all by inhibiting Na_v 1.7 channels to exert analgesic effect.

2.5. Effect of the lead compounds on hERG channels

It was reported that the toxicity of *Aconitum* diterpenoid alkaloids is due to their effect on ion channels. Activation of voltage-gated K⁺ channels is the cause of their cardiotoxicity [67]. Although the compounds designed in this study showed significantly reduced toxicity in animal experiments, their effects on the hERG channel (human-ether-a-go-go-related gene-encoded potassium channel) still need to be tested to determine the potential arrhythmogenic effects. Therefore, we chose Rb⁺ as the tracer ion and evaluated the rubidium efflux ratio, reflecting the block effect on the hERG potassium channel. After adding a high concentration of Rb⁺ buffer to the cultured HEK-hERG cells and incubating for 3 h, the samples to be tested were added, and the cells were incubated for another 4 min. The extra-cellular fluid and cell lysate were collected, and the Rb⁺ ion concentration inside and outside the cell was determined by an ion channel reader (ICR8100, Aurora, Canada). The Rb⁺ ion efflux ratio could reflect the blocking effect of the tested compounds.

As shown in Table 4 and Fig. 6, compounds **35**, **36**, **49**, **70**, and **89** could decrease the Rb⁺ efflux ratio in a concentration-dependent manner, indicating these LA derivatives would inhibit hERG channels. Although these compounds, especially **49**, showed obviously reduced toxicity in acute toxicity experiments in mice, their potassium channel inhibition effects have proved they might own potential risk of arrhythmia. Compound **39** did not show any apparent inhibition of the potassium channel even at the highest test concentration. Based on the above results, we believe **39** from the amide series was the most potential LA derivative that significantly reduced the toxicity of LA without risk of arrhythmia while maintaining the analgesic activity.

3. Conclusion

In summary, inspired by the unique structure of the low toxicity diterpenoid alkaloid we isolated in the previous work, ninety-three LA derivatives were designed and synthesized to find lead compounds with good analgesic activity and low toxicity. The amide series maintained the structural integrity of LA to the greatest extent. The structure modification was only designed and conducted by changing the substituent of the acetamino fragment. A total of forty-five derivatives in three major categories have been synthesized in this series, and three

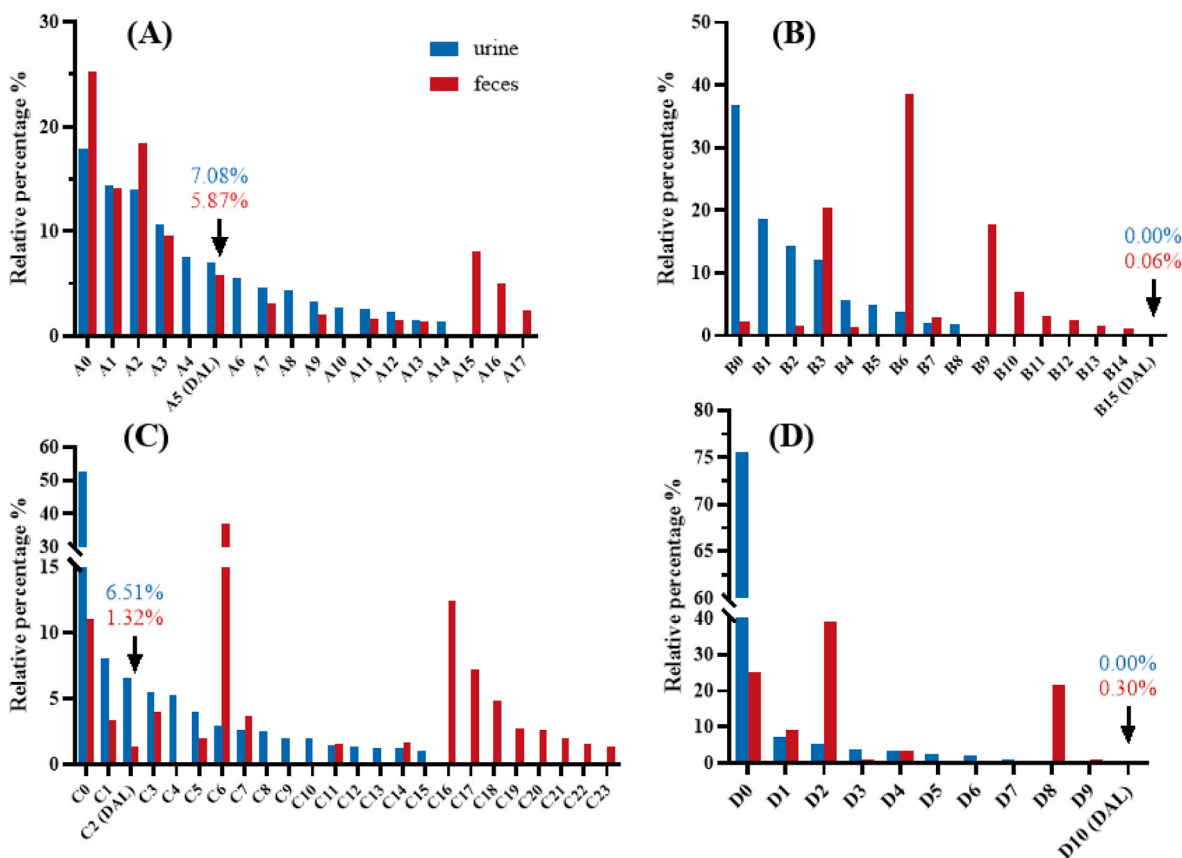


Fig. 4. The relative percentage of all metabolites of compounds 39 (A), 49 (B), 70 (C), and 89 (D) in urine and feces.

Table 3

Li⁺ concentration (ppm) in HEK-Na_v 1.7 cells lysate after treated by LA, 35, 39, 49, 70 and 89 (*n* = 6)^a.

Compounds	0 μM	1 μM	10 μM	100 μM
LA	0.65 ± 0.010	0.63 ± 0.030	0.61 ± 0.020*	0.52 ± 0.010*
35	0.65 ± 0.006	0.60 ± 0.010	0.59 ± 0.010*	0.44 ± 0.020*
39	0.47 ± 0.019	0.49 ± 0.025	0.43 ± 0.027*	0.27 ± 0.037*
49	0.47 ± 0.017	0.47 ± 0.019	0.43 ± 0.002	0.40 ± 0.006*
70	0.63 ± 0.024	0.48 ± 0.031	0.47 ± 0.019	0.46 ± 0.017*
89	0.51 ± 0.021	0.50 ± 0.025	0.47 ± 0.017	0.45 ± 0.013*

^a Values are expressed as the mean ± SEM. **p* < 0.05.

lead compounds, 35, 36, and 39, were screened out. These three compounds were all phenyl-substituted derivatives with electron-donating substituents in the *para* position of the benzene ring. Their low ED₅₀ and high LD₅₀ data indicated that these compounds could be safer analgesics than LA. In addition, the toxicity of compounds 1, 4–6 is equivalent to that of LA, while most of the phenyl-substituted derivatives showed lower toxicity, suggesting the introduction of phenyl substituents might be able to reduce the toxicity of LA derivatives. After converting the amide structure to sulfonamide, a total of forty-eight derivatives from three categories exhibited completely different SAR from the amide series. In the sulfonamide series, three lead compounds were screened out, including compounds 49 and 70 from phenyl-substituted derivatives and compound 89 from heterocyclic-substituted derivatives. These three compounds also reduce their toxicity significantly while maintaining analgesic activity. The toxicity of compound 49 was extremely reduced with its LD₅₀ exceeding 600 mg/kg. The SAR of phenyl-substituted derivatives in both amide series and sulfonamide series was concluded in Fig. 7. Six lead compounds (35, 36, 39, 49, 70, and 89, see Fig. 8) were obtained from synthesized derivatives. Their analgesic activities were equivalent to that of LA, while

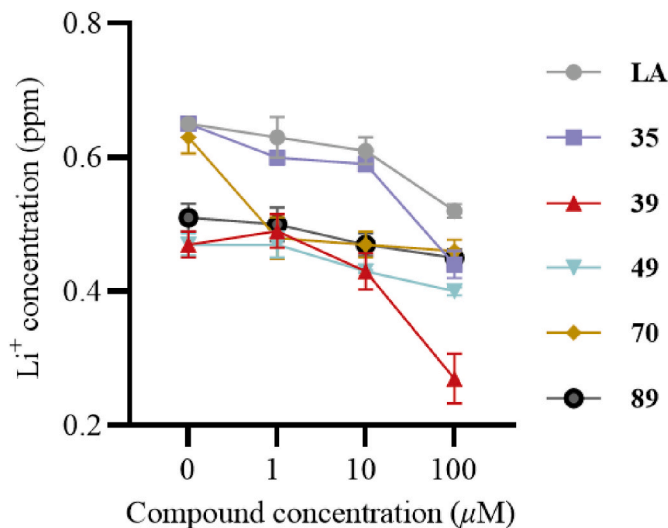


Fig. 5. Effects of compounds on the Li⁺ concentration in HEK-Na_v 1.7 cells lysate.

the toxicity has been significantly reduced, leading to the apparent increase of their therapeutic index.

After screening out six lead compounds (35, 36, 39, 49, 70, and 89) with reduced toxicity, we further conducted an *in vivo* metabolism study to determine the potential toxicity-attenuation mechanism. Although the types of metabolic reactions of the leading compounds and LA were similar, there were significant differences in the amount of the metabolites. DAL, which was abundantly present in the metabolites of LA, exhibited a meager amount in the metabolites of low-toxicity LA

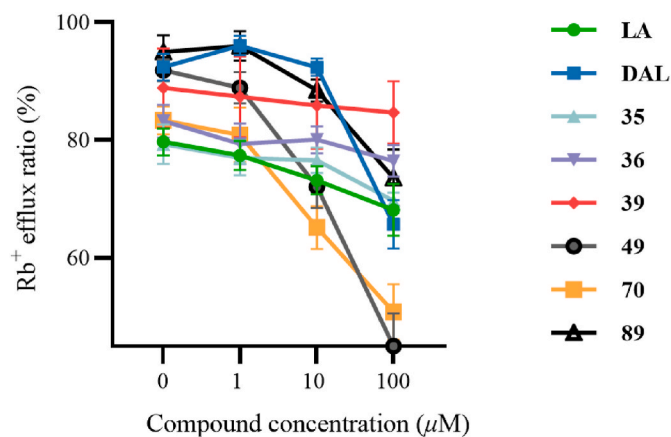


Fig. 6. Effect of the lead compounds on the Rb^+ efflux ratio in hERG channels.

Table 4

Rb^+ efflux ratio (%) of LA, DAL and compounds **35**, **36**, **39**, **49**, **70** and **89** ($n = 6$).

Compounds	0 mg/L	1 mg/L	10 mg/L	100 mg/L
LA	79.71 ± 2.30	77.40 ± 2.47	73.17 ± 2.38*	68.17 ± 4.37*
DAL	92.36 ± 2.27	96.05 ± 1.66	92.35 ± 1.48*	65.70 ± 4.11*
35	79.30 ± 3.34	77.00 ± 2.95	76.58 ± 2.16	69.69 ± 1.37*
36	83.23 ± 2.79	79.38 ± 3.46	80.07 ± 2.30	76.45 ± 2.65*
39	88.85 ± 6.73	87.34 ± 6.84	85.86 ± 7.31	84.70 ± 5.30
49	91.83 ± 1.86	88.87 ± 2.66	72.11 ± 3.68*	44.12 ± 6.45*
70	83.34 ± 2.36	80.88 ± 4.64	65.13 ± 3.63*	50.83 ± 4.70*
89	94.98 ± 2.81	95.97 ± 2.49	88.42 ± 1.87	73.60 ± 4.79*

^a Values are expressed as the mean ± SEM. * $p < 0.05$.

derivatives (**39**, **49**, **70**, and **89**). These facts suggested that DAL might be the primary toxic metabolite of LA and its derivatives. Compounds that were more easily metabolized to DAL *in vivo* were more toxic. Introducing phenyl substituents or replacing the amide bond with a more stable sulfonamide bond to LA was an optimization strategy to reduce the toxicity of LA.

Furthermore, the effects on sodium channels revealed that the analgesic mechanism of these lead compounds was similar to LA, which inhibits the $Na_v 1.7$ channels. In addition, even though the six lead compounds mentioned above showed significantly reduced toxicity in animal experiments, five of them, including compound **49** owned the lowest LD_{50} , could inhibit the hERG channels, which might lead to the potential risk of arrhythmia. Only compound **39** has no potential arrhythmia risk. Thus, depending on all results, compound **39** was

provided as a new analgesic lead compound with activity comparable to that of LA while the toxicity was significantly reduced.

4. Experimental section

4.1. General experimental procedures

1H NMR spectra were recorded on a Bruker AV 400 nuclear magnetic resonance instrument (400 MHz). ^{13}C NMR data were collected on a Bruker AV 400 nuclear magnetic resonance instrument (100 MHz). Chemical shifts were reported in parts per million (ppm) with tetramethylsilane as the internal standard. HRESIMS were determined using a Waters Xevo G2-S Q-ToF mass spectrometer. Reactions were monitored by thin-layer chromatography (TLC) using silica gel GF254 plates, which were visualized by spraying Dragendorff's reagent [41,42]. Reaction products were purified by column chromatography on silica gel (purchased from Qingdao Ocean Chemical Plant) using gradient elution. Acetonitrile and formic acid (HPLC-grade) were purchased from Fisher Scientific Inc. Water was purified using a Milli-Q system (Millipore). Centrifuging was performed by a CENCE H2050R high-speed bench centrifuge. Ion concentration was detected by an ICR8100 ion channel reader (Aurora, Canada). Unless otherwise specified, the reagents and solvents used in this work were commercially available analytical or chemical grades and used directly without any purification.

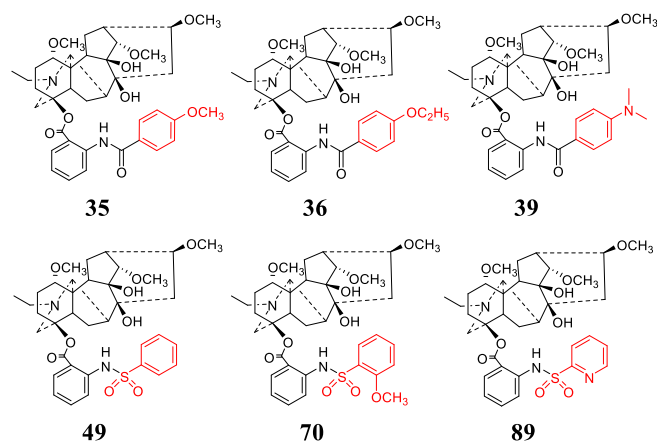


Fig. 8. Six lead compounds of LA derivatives.

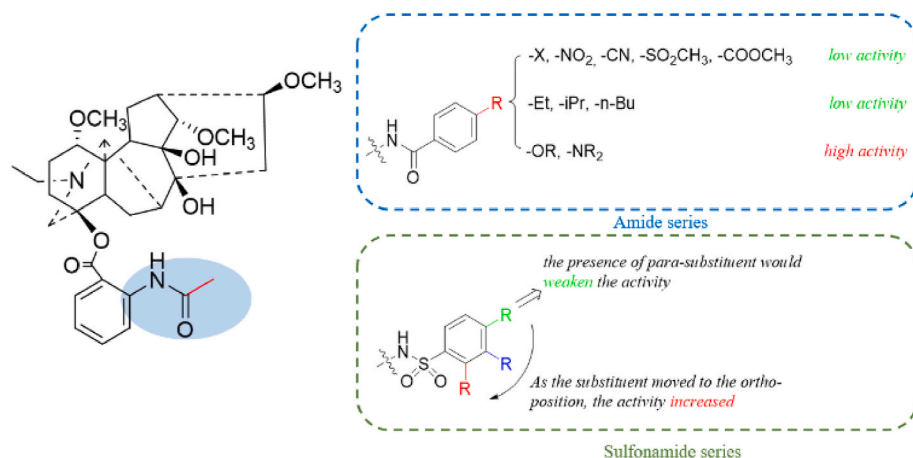


Fig. 7. SAR of phenyl-substituted derivatives.

4.2. Chemical synthesis

4.2.1. Preparation of DAL

2% HCl (15 mL) aqueous solution was slowly added to lappaconitine (1.17 g, 2.0 mmol) at room temperature. The mixture was heated to reflux overnight at 75 °C. After cooling to room temperature spontaneously, a saturated aqueous solution of NaHCO₃ was used to adjust pH to 10, followed by extracting with dichloromethane (3 × 10 mL). The organic layers were combined and washed with brine, dried over Na₂SO₄, and evaporated, giving DAL (1.05 g, yield: 97%) after purification by column chromatography over silica gel (dichloromethane: methanol = 40:1 to 20:1).

4.2.2. General procedure for the synthesis of amide derivatives

4.2.2.1. General procedure for the synthesis of compounds 1–6, 8–9, 14–16, 18, 20, 23–28, 30–32, 36, 39, 42, 44. The corresponding acyl chlorides (2.0–3.0 equivalents) were gently added to a mixture of DAL (100 mg, 0.18 mmol, 1.0 equivalent) in dry dichloromethane (5 mL) and dry pyridine (0.54 mmol, 3.0 equivalents) at 0 °C. The reaction mixture was stirred at room temperature for 2–14 h and monitored by TLC (dichloromethane: methanol = 10: 1). When the starting material was consumed, a saturated aqueous solution of NaHCO₃ was added to adjust the pH of the mixture to 10, followed by extracting with dichloromethane three times. The organic layer was washed with brine, dried over Na₂SO₄, and evaporated to give crude products. These compounds were obtained after being purified by column chromatography over silica gel (dichloromethane: methanol = 40: 1 to 10: 1) in 46–99% yields.

4.2.2.2. General procedure for the synthesis of compounds 7, 10–13, 17, 19, 21–22, 29, 33–35, 37–38, 40–41, 43, 45. Oxalyl chloride (1.5–2.0 equivalents) and *N,N*-dimethylformamide (DMF) were added dropwise to the corresponding carboxylic acid (5.0 equivalents) in dry dichloromethane (5 mL). After 2–4 h, the mixture was evaporated to give the corresponding acid chlorides. The prepared acid chloride and dry pyridine (3.0 equivalents) were added to a solution of DAL (100 mg, 0.18 mmol, 1.0 equivalent) in dry dichloromethane (5 mL) at 0 °C. The mixture was stirred at room temperature. TLC (dichloromethane: methanol = 10: 1) was used to monitor the reaction. After 2–14 h, the reactions were quenched by adding a saturated aqueous solution of NaHCO₃ to adjust the pH to 10. Then the solution was extracted with dichloromethane three times, and the organic layer was washed with brine, dried over Na₂SO₄, and evaporated to give crude products. These compounds were obtained by gradient elution on silica gel (dichloromethane: methanol = 40: 1 to 10: 1) in 17–99% yields.

4.2.3. General procedure for the synthesis of sulfonamide derivatives

4.2.3.1. General procedure for the synthesis of compounds 46–55, 57–88, 90–93. A mixture of DAL (100 mg, 0.18 mmol, 1.0 equivalent) and the appropriate sulfonyl chloride (2.0–3.0 equivalents) in dry dichloromethane (5 mL), together with dry pyridine (0.54 mmol, 3.0 equivalents) was stirred at room temperature for 4–12 h. The reaction was monitored by TLC (dichloromethane: methanol = 10: 1) until DAL disappeared. After adjusting the pH to 10 with a saturated aqueous solution of NaHCO₃, the crude product was provided by evaporating the reaction solution. The mentioned compounds were purified by column chromatography (dichloromethane: methanol = 40:1 to 10: 1) in 39–94% yields.

4.2.3.2. Synthesis of compound 56. Oxalyl Chloride (0.95 mL) was added dropwise to a solution of 4-(dimethylamino)benzenesulfonic acid (752 mg, 3.7 mmol) and DMF (catalyzed amount) in dry dichloromethane at 0 °C. After stirring for 3 h, the reaction mixture was evaporated to give 4-(dimethylamino)benzenesulfonyl chloride. Then 4-(dimethylamino)benzenesulfonyl chloride was added gently to a

solution of DAL (400 mg, 0.73 mmol) and dry pyridine (173 mg, 2.19 mmol). The reaction was stirred at room temperature for 14 h and evaporated to provide crude products. Compound 56 was obtained by column chromatography over silica gel (Petroleum ether: dichloromethane: diethylamine = 20: 1: 1 to 8: 1: 1) as white powder in 8% yield.

4.2.3.3. Synthesis of compound 89. Triethylamine (447 mg, 4.42 mmol) was added portion-wise to a solution of pyridine-2-sulfonic acid (351 mg, 2.21 mmol) in dry dichloromethane at 0 °C and stirred for 15 min. Trifluoromethanesulfonic anhydride (624 mg, 2.21 mmol) was slowly added to the solution. DAL (600 mg, 1.11 mmol) was added to the mixture after 2 h. The reaction was stirred at room temperature for 17 h. The crude product was obtained by evaporating the reaction solvent. Compound 89 (71% yield) was purified by column chromatography over silica gel (Petroleum ether: dichloromethane: diethylamine = 20: 10: 0.3).

4.3. Pharmacology

4.3.1. Experimental animals

Male and female adult (22–25 g body weight) Kunming strain mice (SPF grade) were purchased from Chengdu Dossy Experimental Animals Co., Ltd. (Chengdu, China, License No. SCXK 2020-030). All the animals were housed in plastic cages with thirty mice per cage and thick sawdust bedding in the Southwest Jiaotong University Experimental Animal Center (Chengdu, China) at standard room temperature (22 ± 2 °C), under conditions of a 12/12-h reversed light-dark cycle (7:00 a.m.–7:00 p.m.), and received food and sterilized water ad libitum. Mice were accustomed to the laboratory environment for five days before the experiments. Experimental groups (*n* = 10 in each group) were randomly assigned, and researchers were blinded to the tests.

For *in vivo* metabolism study, three male and three female mice were administered a single dose of the tested compound by subcutaneous injection (50 mg/kg, 0.1 mL/g BW). The control group was administered a similar volume of 0.9% saline.

All the *in vivo* study was approved by the Animal Care and Welfare Committee of Southwest Jiaotong University and carried out under the National Institutes of Health Guide's guidelines for the Care and Use of Laboratory Animals using an approved animal protocol.

4.3.2. Drugs and administration route for mice

All the LA derivatives for the test were dissolved in 0.1 mol/L HCl aqueous solution and diluted with 0.9% saline to the required concentration. It is worth noting that drugs and hydrochloric acid are prepared in terms of equal molar ratios (1:1) to avoid the interference of hydrochloric acid. All the analogues were given by subcutaneous injection 15 min before testing, and 0.7% acetic acid was given by intraperitoneal injection.

4.3.3. *In vivo* analgesic activity

Analgesic activity was performed by the acetic acid-induced writhing test. Ten Kunming mice (half male and half female) were randomly selected and placed separately. All the animals were injected with normal 0.9% saline or LA derivatives solution (0.1 mL/10 kg BW.). The acetic acid solution (0.7%) was given 15 min after drug administration. The number of writhes was recorded as videos and counted during a 15 min period after acetic acid injection. Writhe was defined as the contraction of the abdominal muscles accompanied by elongation of the body and hind limbs. The percentage of inhibition was measured using the following equation: Inhibition (%) of writhing = (Average number of writhing in the control group – Average number of writhing test group)/Average number of writhing in control group × 100%.

ED₅₀ of lead compounds was determined by adapting standard procedures. Kunming mice of either sex were divided into 5 groups of 10 animals each. The test compounds were dissolved in 1, 2, 4, 8, and 16

mg/kg doses and injected. Writhing inhibition in 15 min of each concentration was calculated, and the ED₅₀ data was determined by the probit regression using SPSS (ver. 17.2).

4.3.4. Acute toxicity study

Preliminary toxicity tests were performed by gradually increasing the dose injected until a poisoning reaction or death occurred. LD₅₀ of the lead compounds was determined using standard procedures. Kunming mice of either sex were divided into 5 groups of 10 animals each. The test compounds were dissolved in 50, 100, 200, 400, and 800 mg/kg doses and injected subcutaneously. The toxic symptoms and mortality rates in each group were recorded for 24 h after drug administration. The LD₅₀ data was calculated by probit regression using SPSS (ver. 17.2).

4.4. Metabolism study

4.4.1. Collection and purification of urine and fecal samples

Mice urine and fecal for *in vivo* metabolism study were collected 0–24 h after drug administration in metabolism cages. All samples were frozen at –20 °C until analyzed.

For urine samples, after adding 0.9 mL iced methanol to 0.3 mL urine, the mixture was left to stand for an hour at 4 °C and then vortexed for 3 min and centrifuged at 15000 rpm at 4 °C for 15 min. The supernatant was transferred into a polypropylene centrifuge tube and evaporated to dryness with a gentle flow of nitrogen gas at 45 °C. The residue was redissolved in 1 mL acetonitrile-water (5:95, v/v) and filtered through a 0.22 µm cellulose membrane into an autosampler vial and analyzed by UPLC-TOF-MS.

For fecal samples, each sample was homogenized before weighing. Fecal samples (2 g) were ultrasonically extracted by methanol (8 mL) for 15 min. After settling for 5 min, 0.3 mL supernatant fluid was drawn off, and 0.9 mL iced methanol was added for precipitating proteins. Then the mixture was centrifuged for 15 min at 15000 rpm at 4 °C. The supernatant was transferred into a polypropylene centrifuge tube and quickly blow-dried with nitrogen at 45 °C. The residue was redissolved in 1 mL acetonitrile-water (5:95, v/v) and filtered through a 0.22 µm cellulose membrane into an autosampler vial and analyzed by UPLC-TOF-MS.

4.4.2. Instrument conditions and data analysis

UPLC-Q/TOF-MS^E was equipped with Waters Xevo G2-S Q-TOF mass spectrometer and Waters Acquity UPLC (Waters Corp., Milford, MA, USA). Chromatographic separation of LA metabolites was performed at ambient temperature using an Acquity UPLC HSS T3 column (2.1 × 100 mm, 1.8 µm) (Waters Corp., Milford, MA, USA). The mobile phase comprised 0.1% formic acid in water (solvent A) and acetonitrile (solvent B) and was pumped at a flow rate of 0.4 mL min⁻¹. The gradient elution program was performed as follows: 0–1.0 min, 5% B; 1.0–10.0 min, 5–35% B; 10.0–12.0 min, 35–60% B; 12.0–14.0 min, 60–190% B; 14.0–15.0 min, 90% B; 15.0–15.1 min, 90%–5% B; and 15.1–18.0 min, 5% B. The sample injection volume was 1 µL.

Typical mass spectrometer source conditions used for maximum intensity of precursor ions were as follows: capillary voltage, 1.5 kV; source temperature, 150 °C; desolvation temperature, 500 °C; cone gas (N₂) flow rate, 50 L/h; desolvation gas (N₂) flow rate, 800 Lh⁻¹. The electrospray ionization (ESI) source was operated in the positive ionization mode, and the acquisition analyzer mode was set in sensitivity mode. The acquisition time was 14 min. The data were acquired from *m/z* 50–1000 Da and centroided during acquisition using an internal reference comprised of a 1 ng mL⁻¹ solution of leucine enkephalin infused at 50 µL min⁻¹, generating a reference ion at *m/z* 556.2771 in the ESI positive ionization mode. The scanning time was 0.3 s⁻¹. High-energy data were acquired using a ramp collision energy of 35–55 eV. Data analysis was conducted using the UNIFI scientific information system software (Waters, USA) to rapidly identify metabolites from complex samples.

4.5. Sodium channel test

4.5.1. Reagent for HEK-Nav1.7 cells

The complete medium for HEK-Nav1.7 cells contained Dulbecco's modified eagle medium (DMEM), 10% fetal bovine serum (FBS), and 1% penicillin-streptomycin solution. Sodium-free buffer contained 137 mM choline chloride, 5.4 mM KCl, 0.81 mM MgSO₄, 0.95 mM CaCl₂, 5.5 mM glucose, 25 mM HEPES, pH = 7.4. LiCl buffer contained 45 mM choline chloride, 90 mM LiCl, 5.4 mM KCl, 0.81 mM MgSO₄, 0.95 mM CaCl₂, 5.5 mM glucose, 25 mM HEPES, pH = 7.4. Lysis buffer contained 1% Triton X-100. Li⁺ standard solution was set at 0 ppm, 0.5 ppm, 1 ppm, 2 ppm, 5 ppm, 7.5 ppm, and 10 ppm.

4.5.2. Sodium channel assay procedure

The cell culture plates were coated with 0.1 mg/L poly-D-lysine (PDL) before cell plating and washed twice with ddH₂O. Cells in the logarithmic growth phase were seeded in 96-well plates at a density of 8 × 10⁴ cells/well. After 24 h of adherent growth, remove the cell culture medium, add 200 µL sodium-free buffer and incubate the cells at 37 °C, 5% CO₂ for 15 min. After incubation, discard the sodium-free buffer and cells were treated with compounds dissolved in LiCl-free buffer for 8 min. Then cells were incubated with LiCl buffer containing veratridine (30 µM) and aconitine (50 µM) for 90 min. After the incubation, cells were washed with LiCl-free buffer to remove the extracellular LiCl. Then, cells were lysed by adding 1% Triton X-100 and the absorbance of Li⁺ in cell lysates was measured by ICR8100 at 670.8 nm.

4.6. hERG channel test

4.6.1. Reagent for HEK-hERG cells

The complete medium for HEK-hERG cells contained Dulbecco's modified eagle medium (DMEM), 10% fetal bovine serum (FBS), and 1% penicillin-streptomycin solution. Loading buffer contained 5.4 mM RbCl, 5 mM glucose, 25 mM HEPES, 150 mM NaCl, 1 mM MgCl₂, 0.8 mM NaH₂PO₄, 2 mM CaCl₂, pH = 7.4. Wash buffer contained 5.4 mM KCl, 25 mM HEPES, 150 mM NaCl, 1 mM MgCl₂, 0.8 mM NaH₂PO₄, 2 mM CaCl₂, pH = 7.4. Open buffer contained 30 mM KCl, 25 mM HEPES, 150 mM NaCl, 1 mM MgCl₂, 0.8 mM NaH₂PO₄, 2 mM CaCl₂, pH = 7.4. Lysis buffer contained 1%–1.5% Triton X-100 (diluted with open buffer). Rb⁺ standard solution was set at 0 ppm, 0.5 ppm, 1 ppm, 2 ppm, 5 ppm, 7.5 ppm and 10 ppm.

4.6.2. hERG channel assay procedure

The cell culture plates were coated with 0.1 mg/L poly-D-lysine (PDL) before cell plating and washed twice with ddH₂O. Cells in the logarithmic growth phase were seeded in 96-well plates at a density of 8 × 10⁴ cells/well. After 24 h of adherent growth, remove the cell culture medium, wash the cells with 200 µL loading buffer, add 200 µL loading buffer, and incubate at 37 °C, 5% CO₂ for 3 h. After incubation, discard the loading buffer and wash 3 times with wash buffer. Add 200 µL of drug open buffer to the cells, react for 4 min, then pipette 200 µL of supernatant (extracellular fluid) into a new 96-well plate, add 200 µL of lysis buffer to each well to lyse the cells, and repeat the pipetting to make the cells the lysis is complete. This part of the liquid is intracellular. Using ICR8100 (Aurora, Canada) to measure the absorbance of Rb⁺ in intracellular fluid and extracellular fluid at 780 nm, Rb⁺ outflow ratio = ion concentration of extracellular fluid/(ion concentration of extracellular fluid + ion concentration of intracellular fluid) × 100%.

Declaration of competing interest

The authors declare that they have no known competing financial interests or personal relationships that could have appeared to influence the work reported in this paper.

Data availability

Data will be made available on request.

Acknowledgment

The authors are grateful to NSFC to support this work (Grant NO. 82073734).

Appendix A. Supplementary data

Supplementary data to this article can be found online at <https://doi.org/10.1016/j.ejmech.2022.114776>.

References

- J.M. Hush, M. Nicholas, C.M. Dean, Embedding the IASP Pain curriculum into a 3-year prelicensure physical therapy program: redesigning pain education for future clinicians, *Pain Rep* 3 (2018) e645.
- J. Goesling, L.A. Lin, D.J. Clauw, Psychiatry and pain management: at the intersection of chronic pain and mental health, *Curr. Psychiatr. Rep.* 20 (2018) 12.
- W.M. Hooten, Chronic pain and mental health disorders: shared neural mechanisms, epidemiology, and treatment, *Mayo Clin. Proc.* 91 (2016) 955–970.
- U. Franneby, G. Sandblom, P. Nordin, O. Nyren, U. Gunnarsson, Risk factors for long-term pain after hernia surgery, *Ann. Surg.* 244 (2006) 212.
- P. Baral, S. Udit, I.M. Chiu, Pain and immunity: implications for host defence, *Nat. Rev. Immunol.* 19 (2019) 433–447.
- J.D. Kosiba, S.A. Maisto, J.W. Ditte, Patient-reported use of medical cannabis for pain, anxiety, and depression symptoms: systematic review and meta-analysis, *Soc. Sci. Med.* 233 (2019) 181–192.
- A.J. Means-Christensen, P.P. Roy-Byrne, C.D. Sherbourne, M.G. Craske, M.B. Stein, Relationships among pain, anxiety, and depression in primary care, *Depress. Anxiety* 25 (2008) 593–600.
- W.W. IsHak, R.Y. Wen, L. Naghdechi, B. Vanle, J. Dang, M. Knosp, J. Dascal, L. Marcia, Y. Gohar, L. Eskander, J. Yadegar, S. Hanna, A. Sadek, L. Aguilar-Hernandez, I. Danovitch, C. Louy, Pain and depression: a systematic review, *Harv. Rev. Psychiatr.* 26 (2018) 352–363.
- I. Conejero, E. Olie, R. Calati, D. Ducasse, P. Courtet, Psychological pain, depression, and suicide: recent evidences and future directions, *Curr. Psychiatr. Rep.* 20 (2018) 33.
- E. Petrosky, R. Harpaz, K.A. Fowler, M.K. Bohm, C.G. Helmick, K. Yuan, C.J. Betz, Chronic pain among suicide decedents, 2003 to 2014: findings from the national violent death reporting system, *Ann. Intern. Med.* 169 (2018) 448–455.
- S. Bindu, S. Mazumder, U. Bandyopadhyay, Non-steroidal anti-inflammatory drugs (nsaids) and organ damage: a current perspective, *Biochem. Pharmacol.* 180 (2020) 114–147.
- A. Fernandez, I. Kirsch, L. Noel, P.Y. Rodondi, T.J. Kaptchuk, M.R. Suter, I. Decosterd, C.A. Berna, Test of positive suggestions about side effects as a way of enhancing the analgesic response to NSAIDs, *PLoS One* 14 (2019), e0209851.
- G. Garcia-Rayado, M. Navarro, A. Lanas, NSAID induced gastrointestinal damage and designing gi-sparing NSAIDs, *Expet Rev. Clin. Pharmacol.* 11 (2018) 1031–1043.
- D.A. Nelson, E.S. Marks, P.A. Deuster, F.G. O'Connor, L.M. Kurina, Association of nonsteroidal anti-inflammatory drug prescriptions with kidney disease among active young and middle-aged adults, *JAMA Netw. Open* 2 (2019), e187896.
- M. Baker, M.A. Perazella, NSAIDs in CKD: are they safe? *Am. J. Kidney Dis.* 76 (2020) 546–557.
- O.J. Kweon, Y.K. Lim, B. Kim, M.K. Lee, H.R. Kim, Effectiveness of platelet function analyzer-100 for laboratory detection of anti-platelet drug-induced platelet dysfunction, *Ann. Lab. Med.* 39 (2019) 23–30.
- A.M. Schjerning, P. McGettigan, G. Gislason, Cardiovascular effects and safety of non-aspirin NSAIDs, *Nat. Rev. Cardiol.* 17 (2020) 574–584.
- C.J. Pepine, P.A. Gurbel, Cardiovascular safety of NSAIDs: additional insights after precision and point of view, *Clin. Cardiol.* 40 (2017) 1352–1356.
- A.E. Conibear, E. Kelly, A biased view of mu-opioid receptors, *Mol. Pharmacol.* 96 (2019) 542–549.
- J.A. Radcliff, R.M. Rafeq, J.F. Bowen, L. Pontiggia, S. Sen, Predictors of response in emergency department patients receiving intravenous opioids for severe pain, *Pharmacotherapy* 37 (2017) 799–805.
- P.J. Wiffen, B. Wee, S. Derry, R.F. Bell, R.A. Moore, Opioids for cancer pain - an overview of cochrane reviews, *Cochrane Db. Syst. Rev.* 7 (2017) CD012592.
- L.B. Gerlach, M. Olsson, H.C. Kales, D.T. Maust, Opioids and other central nervous system-active polypharmacy in older adults in the United States, *J. Am. Geriatr. Soc.* 65 (2017) 2052–2056.
- Z. Liu, C. C Udenigwe, Role of food-derived opioid peptides in the central nervous and gastrointestinal systems, *J. Food Biochem.* 43 (2019), e12629.
- N.D. Volkow, E.B. Jones, E.B. Einstein, E.M. Wargo, Prevention and treatment of opioid misuse and addiction: a review, *JAMA Psychiatr.* 76 (2019) 208–216.
- C. Eiden, O. Mathieu, H. Donnadiu-Rigole, C. Marrot, H. Peyriere, High opioids tolerance due to transmucosal fentanyl abuse, *Eur. J. Clin. Pharmacol.* 73 (2017) 1195–1196.
- X. Lin, A.S. Dhopeswarkar, M. Huibregtse, K. Mackie, A.G. Hohmann, Slowly signaling G protein-biased CB2 cannabinoid receptor agonist LY2828360 suppresses neuropathic pain with sustained efficacy and attenuates morphine tolerance and dependence, *Mol. Pharmacol.* 93 (2018) 49–62.
- P. Esmaili-Shahzade-Ali-Akbari, H. Hosseinzadeh, S. Mehri, Effect of suvorexant on morphine tolerance and dependence in mice: role of NMDA, AMPA, ERK and CREB proteins, *Neurotoxicology* 84 (2021) 64–72.
- H.D. de Boer, O. Detriche, P. Forget, Opioid-related side effects: postoperative ileus, urinary retention, nausea and vomiting, and shivering: a review of the literature, *Best Pract. Res. Clin. Anaesthesiol.* 31 (2017) 499–504.
- A.D. Farmer, C.B. Holt, T.J. Downes, E. Ruggeri, S. Del Vecchio, R. De Giorgio, Pathophysiology, diagnosis, and management of opioid-induced constipation, *Lancet Gastroenterol* 3 (2018) 203–212.
- M.C. Bicket, J.J. Long, P.J. Pronovost, G.C. Alexander, C.L. Wu, Prescription opioid analgesics commonly unused after surgery: a systematic review, *JAMA Surg* 152 (2017) 1066–1071.
- W. Zhu, M.E. Cherner, T.B. Sherry, N. Maestas, Initial opioid prescriptions among U.S. commercially insured patients, 2012–2017, *N. Engl. J. Med.* 380 (2019) 1043–1052.
- S. Ali, R. Chouhan, P. Sultan, Q.P. Hassan, S.G. Gandhi, A comprehensive review of phytochemistry, pharmacology and toxicology of the genus *Aconitum L.*, *Adv. Tradit. Med.* (2021) 1–22.
- A. Shoaib, H.H. Siddiqui, R.K. Dixit, S. Siddiqui, B. Deen, A. Khan, S.H. Alrokayan, H.A. Khan, P. Ahmad, Neuroprotective effects of dried tubers of *Aconitum Napellus*, *Plants-Basel.* 9 (2020) 356.
- L. Zhang, T. Li, R. Wang, J. Xu, L. Zhou, L. Yan, Z. Hu, H. Li, F. Liu, W. Du, P. Tong, H. Wu, S. Zhang, L. Shan, T. Efferth, Evaluation of long-time decoction-detoxicated hei-shun-pian (processed *Aconitum Carmichaeli Debeaux* lateral root with peel) for its acute toxicity and therapeutic effect on mono-iodoacetate induced osteoarthritis, *Front. Pharmacol.* 11 (2020) 1053.
- M.Y. Ren, Q.T. Yu, C.Y. Shi, J.B. Luo, Anticancer activities of C18-, C19-, C20-, and bis-diterpenoid alkaloids derived from genus *Aconitum*, *Molecules* 22 (2017) 267.
- N. Ablajan, B. Zhao, J.Y. Zhao, B.L. Wang, S.S. Sagdullaev, H.A. Aisa, Diterpenoid alkaloids from *Aconitum Barbatum* var. *Puberulum Ledeb.*, *Phytochemistry* 181 (2021), 112567.
- P. Cai, H. Qiu, F. Qi, X. Zhang, The toxicity and safety of traditional Chinese medicines: please treat with rationality, *Biosci, Trends* 13 (2019) 367–373.
- M. Tang, W. Zhao, M. Xing, J. Zhao, Z. Jiang, J. You, B. Ni, Y. Ni, C. Liu, J. Li, X. Chen, Resource allocation strategies among vegetative growing, sexual reproduction, a sexual reproduction and defense during growth season of *Aconitum Kusnezoffii Reichb.*, *Plant J.* 105 (2021) 957–977.
- Y. Shen, W.J. Liang, Y.N. Shi, E.J. Kennelly, D.K. Zhao, Structural diversity, bioactivities, and biosynthesis of natural diterpenoid alkaloids, *Nat. Prod. Rep.* 37 (2020) 763–796.
- Y.Z. Li, L.L. Qin, F. Gao, L.H. Shan, X.L. Zhou, Kusnezosines A-C, three C19-diterpenoid alkaloids with a new skeleton from *Aconitum Kusnezoffii Reichb. var. Gibbiferum*, *Fitoterapia* 144 (2020), 104609.
- L.X. Wan, J.F. Zhang, Y.Q. Zhen, L. Zhang, X. Li, F. Gao, X.L. Zhou, Isolation, structure elucidation, semi-synthesis, and structural modification of C19-diterpenoid alkaloids from *Aconitum Apetalum* and their neuroprotective activities, *J. Nat. Prod.* 84 (2021) 1067–1077.
- X. Zhang, Y.S. Shang, F. Gao, D.M. Fang, X.H. Li, X.L. Zhou, Synthesis and evaluation of a series of new bulleyaconitine A derivatives as analgesics, *ACS Omega* 5 (2020) 21211–21218.
- K. Fu, M. Xu, Y. Zhou, X. Li, Z. Wang, X. Liu, X. Meng, Y. Zeng, H. Zhang, The status quo and way forwards on the development of Tibetan medicine and the pharmacological research of Tibetan materia, *Medica, Pharmacol. Res.* 155 (2020), 104688.
- F. Pereira, Polypharmacology of *Aconitum* and *Delphinium* sp. diterpene alkaloids: antiarrhythmic, analgesic and anti-inflammatory effects, *Mini-Reviews Org. Chem.* 14 (2017) 304–310.
- T.F. Li, H. Fan, Y.X. Wang, Aconitum-derived bulleyaconitine A exhibits anti-hypersensitivity through direct stimulating dynorphin A expression in spinal microglia, *J. Pain* 17 (2016) 530–548.
- Q. Huang, X.F. Mao, H.Y. Wu, T.F. Li, M.L. Sun, H. Liu, Y.X. Wang, Bullatine A stimulates spinal microglial dynorphin A expression to produce anti-hypersensitivity in a variety of rat pain models, *J. Neuroinflammation* 13 (2016) 214.
- T.F. Li, H.Y. Wu, Y.R. Wang, X.Y. Li, Y.X. Wang, Molecular signaling underlying bulleyaconitine A (BAA)-induced microglial expression of prodynorphin, *Sci. Rep.* 7 (2017) 45–56.
- W. Huang, S. Ou, Research progress on analgesia of auridin hydrobromide (in Chinese), *Chin. J. Hyg. Res.* 2 (2016) 377–381.
- G. Teng, X. Zhang, C. Zhang, L. Chen, W. Sun, T. Qiu, J. Zhang, Lappaconitine trifluoroacetate contained polyvinyl alcohol nanofibrous membranes: characterization, biological activities and transdermal application, *Mat. Sci. Eng. C-Mater.* 108 (2020), 110515.
- J.H. Lee, Y.K. Lee, H.J. Lee, J.S. Kim, The analgesic effect of *aconitum sinomontanum nakai* pharmacopuncture in sprague-dawley rats, *J. Acup. Res.* 38 (2021) 140–145.
- D. Qu, X. Zhang, C. Sang, Y. Zhou, J. Ma, L. Hui, Lappaconitine sulfate induces apoptosis in human colon cancer HT-29 cells and down-regulates PI3K/AKT/GSK3 β signaling pathway, *Med. Chem. Res.* 28 (2019) 907–916.
- F.N. Dzhabkhangirov, M.N. Sultankhodzhaev, B. Tashkho-dzhaev, Diterpenoid alkaloids as a new class of antiarrhythmic agents. structure-activity relationship, *Chem. Nat. Compd.* 33 (1997) 190–202.

- [53] F.N. Dzhakhgairov, K.R. Kasymova, M.N. Sultankhodzhaev, Toxicity and local anesthetic activity of diterpenoid alkaloids, *Chem. Nat. Compd.* 43 (2007) 581–589.
- [54] Y.R. Sheikh-Zade, I.L. Cherednik, P.A. Galenko-Yaroshevskii, Peculiarities of cardiotropic effect of aconitine, *Bull. Exp. Biol. Med.* 129 (2000) 365–366.
- [55] W. Sun, Z. Shi, H. Wang, Synthesis, characterization and antinociceptive properties of the lappaconitine salts, *Med. Chem. Res.* 24 (2015) 3474–3482.
- [56] M. Angélica, A. Nava-Ocampo, The local anesthetic activity of *aconitum* alkaloids can be explained by their structural properties: a QSAR analysis, *Fund. Clin. Pharmacol.* 18 (2004) 157–161.
- [57] J. Wang, X. Shen, Q. Chen, Structure–analgesic activity relationship studies on the C18- and C19-diterpenoid alkaloids, *Chem. Pharm. Bull.* 57 (2009) 801–807.
- [58] A. Ameri, The effects of *Aconitum* alkaloids on the central nervous system, *Prog. Neurobiol.* 56 (1998) 211–235.
- [59] C. Wang, D. Sun, C. Liu, C. Zhu, X. Jing, S. Chen, C. Liu, K. Zhi, T. Xu, H. Wang, J. Liu, Y. Xu, Z. Liu, N. Lin, Mother root of *Aconitum Carmichaelii Debeaux* exerts antinociceptive effect in complet freund’s adjuvant-induced mice: roles of dynorpin/kappa-opioid system and transient receptor potential vanilloid type-1 ion channel, *J. Transl. Med.* 13 (2015) 1–13.
- [60] M.X. Wang, W. Li, Y. Wang, Y.B. Song, J. Wang, M.S. Cheng, In silico insight into voltage-gated sodium channel 1.7 inhibition for anti-pain drug discovery, *Bioorgan, J. Mol. Graph. Model.* 84 (2018) 18–28.
- [61] P. Siebenga, G. van Amerongen, J.L. Hay, A. McDonnell, D. Gorman, R. Butt, G. J. Groeneveld, Lack of detection of the analgesic properties of PF-05089771, a selective Nav 1.7 inhibitor, using a battery of pain models in healthy subjects, *Clin. Transl. Sci.* 13 (2020) 318–324.
- [62] S. Yang, H. Zhang, R.C. Beier, F. Sun, X. Cao, J. Shen, Z. Wang, S. Zhang, Comparative metabolism of lappaconitine in rat and human liver microsomes and in vivo of rat using ultra high-performance liquid chromatography-quadrupole/time-of-flight mass spectrometry, *J. Pharmaceut. Biomed.* 110 (2015) 1–11.
- [63] F. Xie, H. Wang, H. Shu, J. Li, J. Jiang, J. Chang, Y. Hsieh, Separation and characterization of the metabolic products of lappaconitine in rat urine by high-performance liquid chromatography, *J. Chromatogr. B* 526 (1990) 109–118.
- [64] M. Wang, Y. Wang, D. Kong, H. Jiang, J. Wang, M. Cheng, In silico exploration of aryl sulfonamide analogs as voltage-gated sodium channel 1.7 inhibitors by using 3D-QSAR, molecular docking study, and molecular dynamics simulations, *Comput. Biol. Chem.* 77 (2018) 214–225.
- [65] M. Arpad, P. Lukacs, The enigmatic drug binding site for sodium channel inhibitors, *Curr. Mol. Pharmacol.* 3 (2010) 129–144.
- [66] Y. Li, Y. Zheng, Y. Yu, Y. Gan, Z. Gao D, Inhibitory effects of lappaconitine on the neuronal isoforms of voltage-gated sodium channels, *Acta Pharmacol. Sin.* 40 (2019) 451–459.
- [67] T. Kiss, B. Borcsa, P. Orvos, L. Tálosi, J. Hohmann, D. Csupor, Diterpene lipo-alkaloids with selective activities on cardiac K⁺ channels, *Planta Med.* 83 (2017) 1321–1328.